Theoretical study of silicon–sulfur clusters (SiS2)n– (n=1–6)

ARTICLE *in* INTERNATIONAL JOURNAL OF QUANTUM CHEMISTRY · FEBRUARY 2001

Impact Factor: 1.43 · DOI: 10.1002/1097-461X(2001)81:4<280::AID-QUA5>3.0.CO;2-E

6 AUTHORS, INCLUDING:

Sufan Wang
Anhui Normal University
61 PUBLICATIONS **489** CITATIONS

SEE PROFILE

Theoretical Study of Silicon–Sulfur Clusters $(SiS_2)_n^-$ ($n = 1$–6)

SU-FAN WANG,[1] JI-KANG FENG,[1] CHIA-CHUNG SUN,[1] PENG LIU,[2] ZHEN GAO,[2] FAN-AO KONG[2]

[1]*State Key Laboratory of Theoretical and Computational Chemistry, Institute of Theoretical Chemistry, Jilin University, Changchun, 130023*
[2]*State Key Laboratory of Molecular Reaction Dynamic, Institute of Chemistry, Chinese Academy of Science, Beijing, 100080*

Received 6 July 1999; revised 27 September 2000; accepted 28 September 2000

ABSTRACT: The possible geometrical structures and relative stability of silicon–sulfur clusters (SiS_2) ($n = 1$–6) are explored by means of density functional theory (DFT) quantum chemical calculations. We also compare DFT with second-order Møller–Plesset (MP2) and Hartree–Fock (HF) methods. The effects of polarization functions, diffuse functions, and electron correlation are included in MP2 and B3LYP quantum chemical calculations, and B3LYP is effective in larger cluster structure optimization, so we can conclude that the DFT approach is useful in establishing trends. The electronic structures and vibrational spectra of the most stable geometrical structures of $(SiS_2)_n^-$ are analyzed by B3LYP. As a result, the regularity of the $(SiS_2)_n^-$ cluster growing is obtained, and the calculation may predict the formation mechanism of the $(SiS_2)_n^-$ cluster. Int J Quantum Chem 81: 280–290, 2001

Key words: silicon–sulfur clusters; geometry; electronic structure; vibrational spectra

Introduction

Silicon is one of the most abundant elements on the earth. Its importance in science and technology results from its diverse usage ranging from glass to catalysis to Si-based microelectronic devices and optical fiber communications. That is why silicon clusters have been the focus of a series of experimental and theoretical studies. With the development of the computer and the algorithms of quantum chemistry, more and more theoretical studies were reported and which would even give some predictions before experiment. Related calculations to silicon clusters have proved to be invaluable in understanding the various experimental phenomena of silicon clusters. For example, Raghavachari and Rohlfing [1, 2] calculated the geometry and vibrational frequencies of neutral silicon clusters and anions of silicon clusters before any relative experiments. A series of theoretical studies on binary clusters containing silicon, such as

Correspondence to: J.-K. Feng; e-mail: itcilu@public.cc.jl.cn.
Contract grant sponsor: National Natural Science Foundation of China.

Si–Na [3, 4], Si–F [5], Si–O [6–8], and so on, have been carried out in the last decade.

Sulfur has the largest number of allotropes of any element. The study of the geometric and electronic structure of sulfur is very important in investigating properties and applications of it. Much attention was paid to sulfur clusters and binary clusters containing sulfur. Hohl and Raghavachari and coworkers [9, 10] investigated the geometric of and electronic structures of sulfur clusters. The binary clusters such as C–S [11, 12], Ag–S [13, 14], and W–S [15] have been explored with quantum chemistry methods.

Recently, silicon–sulfur cluster anions and cations have been produced. And now in this work we calculate $(SiS_2)_n^-$ (n = 1–6) clusters and predict the formation mechanism of the $(SiS_2)_n^-$ cluster.

Experimental Results

Silicon–sulfur cluster anions and cations have been produced using direct laser ablation on a solid sample containing a mixture of sulfur and silicon powder. The photodissociation of the clusters was studied with a tandem time-of-flight (TOF) mass spectrometer. There are many intense peaks of cluster anions and cations in the mass spectra, such as $(SiS_2)_n^{\pm}$, $[(SiS_2)_nS]^{\pm}$, $[(SiS_2)_nSiS]^+$, $[(SiS_2)_nSi_6S]^-$, $[(SiS_2)_nSi_6]^-$, etc. And $(SiS_2)_n^-$ are the more intense peaks (Fig. 1). We also studied the mass spectra of the small mass clusters distribution and found that the peaks of $(SiS_2)_n^-$ ($n = 1, 2$) are the more intense ones also. It indicates that $(SiS_2)_n^-$ clusters are more stable clusters. From the results of the experiment,

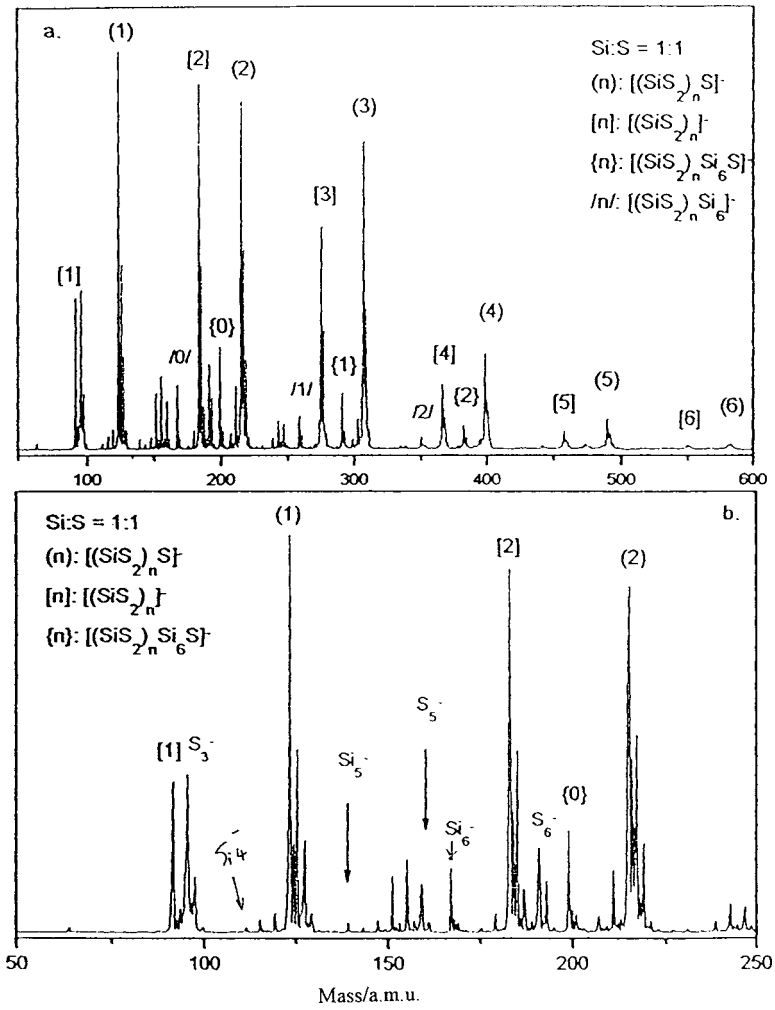

FIGURE 1. TOF mass spectra of Si/S cluster ions produced by laser ablation of mixture of Si and S (Si:S = 1:1).

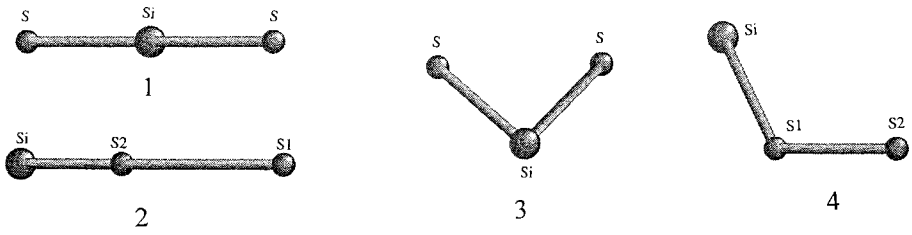

FIGURE 2. Geometrical structures of SiS_2^- isomers.

we may predict that when the powders of silicon and sulfur are mixed together, as the laser energy was added, silicon and sulfur atoms reacted and produced SiS_2^-, while with the energy increased, more and more silicon and sulfur atoms gather and form $(SiS_2)_n^-$. In this work we calculate $(SiS_2)_n^-$ ($n = 1$–6) clusters by quantum chemistry method and predict the formation mechanism of the $(SiS_2)_n^-$ cluster.

Computational Details

The geometric and electronic structures of the $(SiS_2)_n^-$ ($n = 1, 2$) cluster ions were studied by means of unrestricted Hartree–Fock (HF), B3LYP [16–18], and second-order Møller–Plesset (MP2) with polarized and diffuse function 6-31+G* basis set [19–23] available in the GAUSSIAN94 package [24]. In general there are not severe discrepancies between the HF, MP2, and B3LYP geometric parameters and the equilibrium geometry is close. Both MP2 and B3LYP include electron correlation, but B3LYP is effective in larger cluster structure optimization, so we can conclude that the density functional theory (DFT) approach is useful in establishing trends. There also have been many theoretical studies indicating that DFT is reliable in the geometry optimization of binary clusters containing silicon or sulfur [25–28]. In this studys the geometric and electronic structures of the $(SiS_2)_n^-$ cluster ions and the harmonic vibrational frequencies of the most stable isomers were studied by means of unrestricted DFT. The standard three-parameter Becke exchange functional with the Lee, Yang, and Parr non-local correlation function (B3LYP).

Individual Clusters

SiS_2^-

SiS_2^- the smallest one, can be regarded as the core of $(SiS_2)_n^-$ clusters. In Figure 2, the possible geometries of the SiS_2^- clusters are given. The parameters of SiS_2^- optimized by HF, MP2, and B3LYP are shown in Table I. The bond lengths

TABLE I
Geometric parameters (bond length in Å, bond angle in degrees) of SiS_2^- optimized by HF, MP2, and B3LYP.

Structure	Symmetry	State	Geometrical parameter	Optimized value		
				HF	MP2	B3LYP
1	$D_{\infty h}$	$^2\Sigma_g$	Si–S	2.023	2.020	2.065
2	$C_{\infty v}$	$^2\Sigma_g$	Si–S2	2.0435	1.942	1.962
			S1–S2	2.1377	3.589	3.117
3	C_{2v}	$^2B_2$	Si–S	2.099	2.097	2.127
			S–Si–S	91.794	90.669	92.199
4	C_s	$^2A'$	Si–S1	2.070	2.070	2.093
			S1–S2	2.110	2.078	2.111
			S2–S1–Si	112.577	115.817	117.927

and bond angles do not have severe discrepancies among the three methods. In general, the bond lengths are longer and the bond angles larger by B3LYP. But in structure (2) is a special case with HF, the bond length of S1–S2 is 2.138 Å, much shorter than 3.589 Å in MP2, or 3.117 Å in B3LYP. Even though the binding of S–S is greater by HF, the total energy is very high, and there are imaginary frequencies. So we can infer that the electron correction is very important in the $(SiS_2)_n^-$ cluster. By MP2 and B3LYP, the Si–S bond lengths in structure (1) and (3) are similar. There are S–S bonds in (2) and (4), but the S–S bond length of (2) is longer than 3 Å, the binding is very weak, the bond is likely broken, so (2) is not a stable structure, and this conclusion can be provided by its vibrational spectrum, which has an imaginary frequency. All the three methods indicate that structures (3) and (4) are equilibrium structures, and structure (3) is the more stable one, which has symmetry of C_{2v}, the electronic state is $^2B_2$. Vibrational analysis reveals that the $^2B_2$ state is a true minimum on the SiS_2^- potential energy surface. But the vibrational frequencies of structure (1) are all positive with the MP2 method, so one can infer that structure (1) is another equilibrium structure under the MP2 level.

$(SiS_2)_2^-$

$(SiS_2)_2^-$ can be regarded as the dimer of SiS_2 and SiS_2^- with the binding of Si–S, Si–Si, and S–S as shown in Figure 3. The structures of $(SiS_2)_2^-$ are also optimized by HF, MP2, and B3LYP and the geometric parameters are, respectively, shown in Table II for comparison. There are no severe discrepancies among the bond lengths by these three methods. It can be seen from the total energy of all three methods that the most stable structure is (5), which has C_{2v} symmetry, and it is the only structure for which frequen-

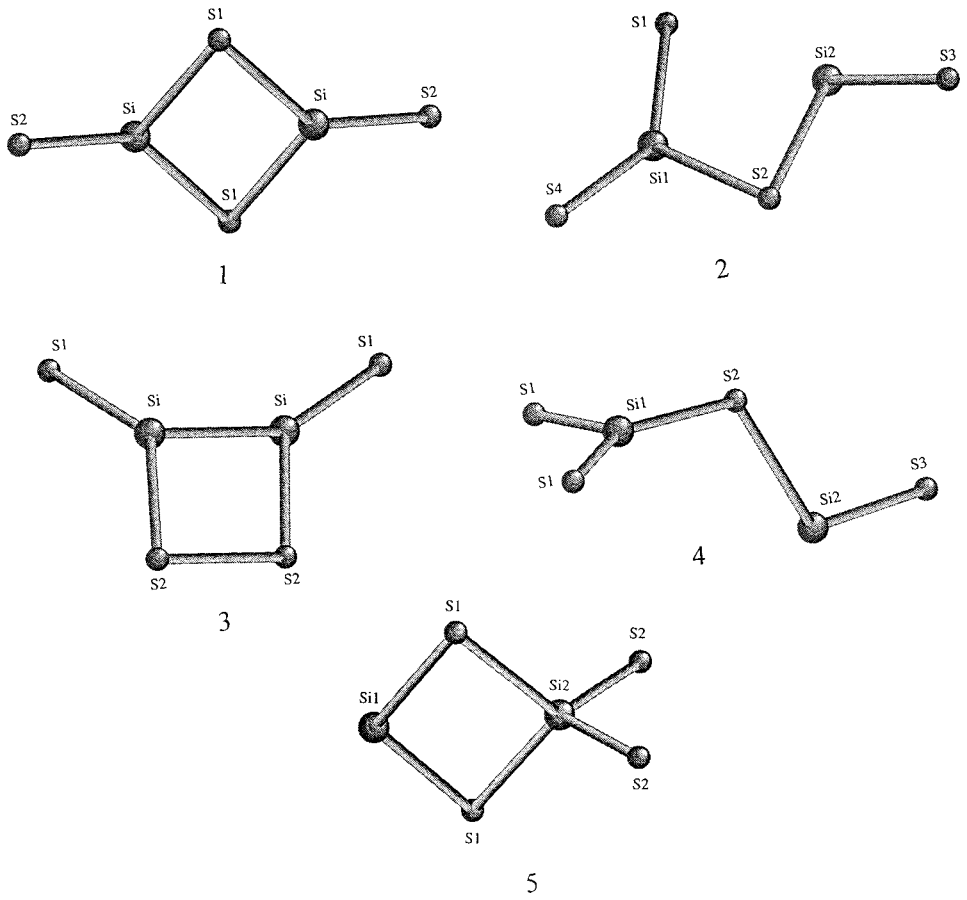

FIGURE 3. Geometrical structures of $(SiS_2)_2^-$ isomers.

TABLE II
Geometric parameters (bond length in Å) of $(SiS_2)_2^-$ optimized by HF, MP2, and B3LYP.

Structure	Symmetry	State	Geometrical parameter	Optimized value		
				HF	MP2	B3LYP
1	D_{2h}	^2A_g	Si–S1	2.156	2.174	2.216
			Si–S2	1.963	1.986	2.013
2	$C_{s(1)}$	$^2A'$	Si1–S1	1.986	2.026	2.050
			Si1–S2	2.208	2.159	2.039
			Si1–S4	1.974	1.977	2.046
			Si2–S2	2.112	2.160	2.356
			Si2–S3	1.968	1.995	1.981
3	$C_{2v(1)}$	$^2B_1$	Si–S1	1.978	1.984	2.000
			Si–S2	2.179	2.183	2.209
			Si–Si	2.229	2.252	2.257
			S2–S2	2.106	2.119	2.143
4	$C_{s(2)}$	$^2A''$	Si1–S1	2.029	2.028	2.038
			Si1–S2	2.005	2.019	2.050
			Si2–S2	2.876	2.626	2.651
			Si2–S3	1.953	1.982	1.999
5	$C_{2v(2)}$	$^2B_1$	Si1–S1	2.139	2.137	2.167
			Si2–S1	2.200	2.195	2.229
			Si2–S2	2.058	2.053	2.075

cies are all positive. The difference from other structures is that the charges on Si1, S1, and S2 are all negative. From this result, we can conclude that there is stronger covalent binding in the most stable structure of $(SiS_2)_2^-$. In the structure with C_{2v} symmetry of $(SiS_2)_2^-$, the electronic state is $^2B_1$.

$(SiS_2)_3^-$

We designed the structures of trimer with the same scheme, as constructing of the dimer, that is, the binding of Si–S is the main binding effect among monomers. The structures optimized by B3LYP are shown in Figure 4. The energy stability order is obtained as (5) > (4) > (2) > (1) > (3). We find that trimer trends to be of the tetratomic ring structure with the rings perpendicular to each other, but for structure (4), even if its total energy is very low, but there is an imaginary frequency in its theoretical vibrational analysis, so it is not the candidate of stable structure of $(SiS_2)_3^-$. The most stable structure of $(SiS_2)_3^-$ is the tetratomic rings structure (5) with C_{2v} symmetry with $^2A_1$ electronic state.

$(SiS_2)_4^-$

The optimized geometrical structures of $(SiS_2)_4^-$ by B3LYP are shown in Figure 5. The energy stability order is (5) > (2) > (4) > (1) > (3). The difference among these five structures is that the rings in structures (2), (4), and (5) are perpendicular to each other, while the rings in (1) and (3) are co-planar. It indicates that if all S atoms binding to the Si atoms are all in the same plane, there will be a large repulsion between S atoms, so the structures will be unstable. But there are imaginary frequencies in the vibrational analysis of structures (4) and (2), so structure (5) with C_{2v} symmetry is the only most stable structure of $(SiS_2)_4^-$, and the electronic state is $^2A_2$.

$(SiS_2)_5^-$, $(SiS_2)_6^-$

Based on the conclusions from geometric structures of $(SiS_2)_n^-$ (n = 1–4), we may conclude that the most stable structure of $(SiS_2)_n^-$ has C_{2v} symmetry, and the formation regularity is that basing the structure of SiS_2^- with C_{2v} symmetry adding

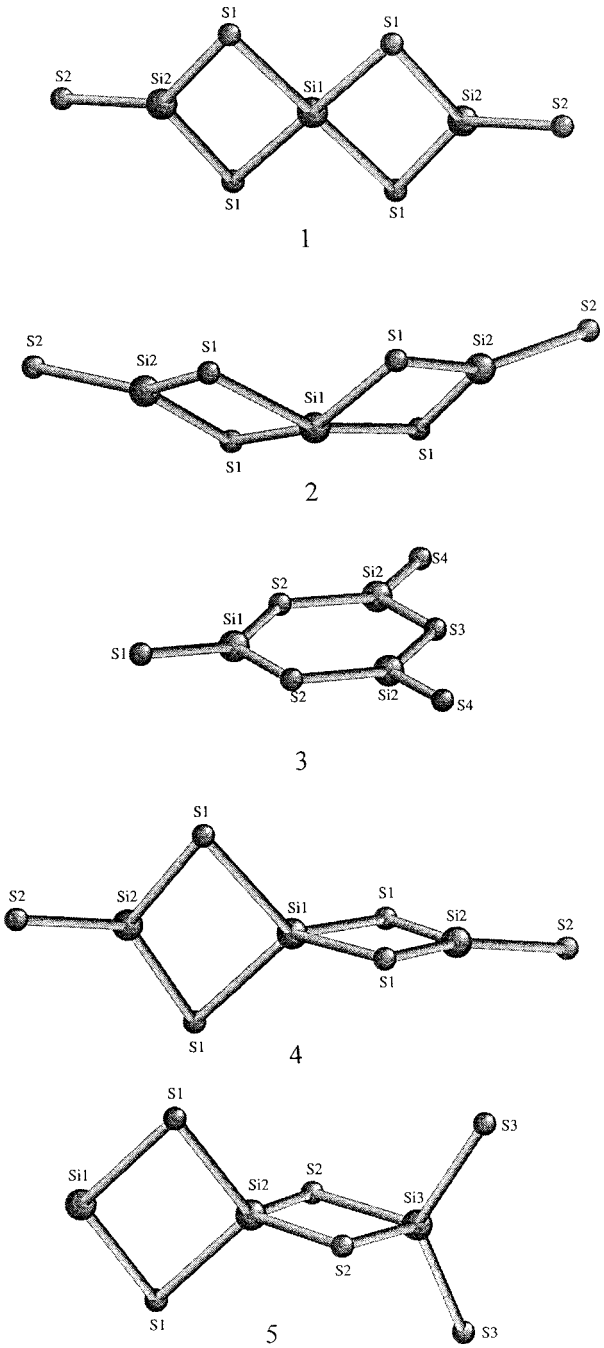

FIGURE 4. Geometrical structures of $(SiS_2)_3^-$ isomers.

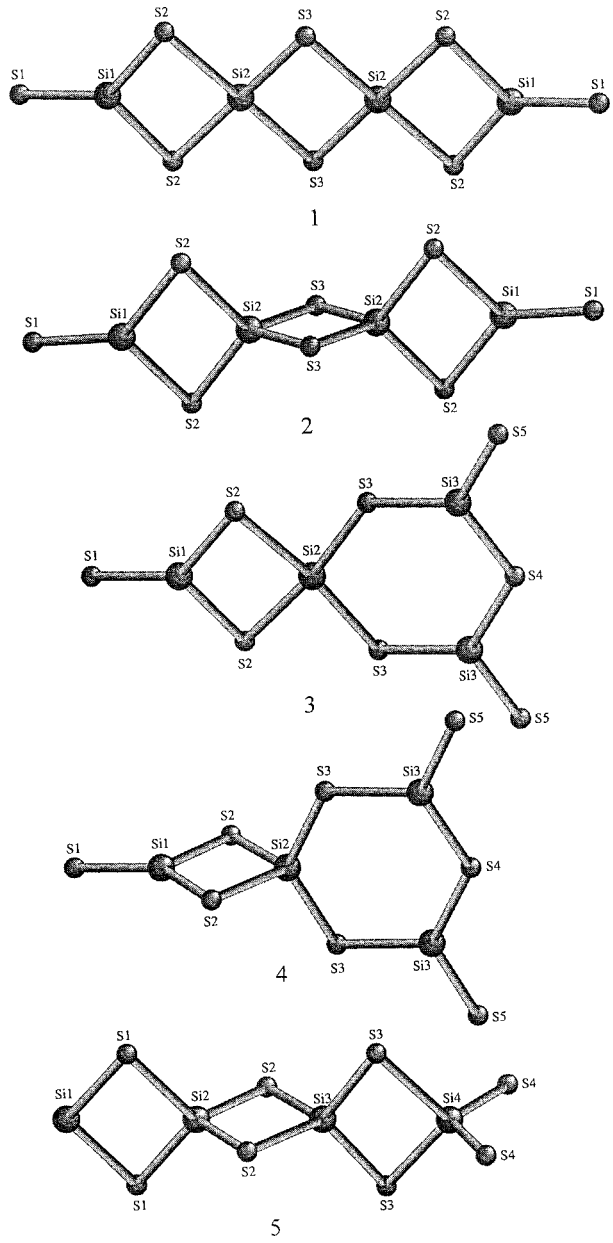

FIGURE 5. Geometrical structures of $(SiS_2)_4^-$ isomers.

units of SiS_2 through the binding of the two S atoms with Si atom forming tetratomic rings perpendicular to each other. So we designed pentamer $(SiS_2)_5^-$ and hexamer $(SiS_2)_6^-$ according to this regularity shown as Figure 6. Vibrational frequencies are all positive for (1) and (2) under the B3LYP method, so the structures with C_{2v} symmetry of $(SiS_2)_5^-$, $(SiS_2)_6^-$ are stable structures. And this result provides the regularity of $(SiS_2)_n^-$ formation.

Results and Discussion

The geometric and electronic structures of $(SiS_2)_n^-$ $(n = 1,2)$ cluster ions were studied by means of unrestricted HF, DFT/B3LYP, and MP2

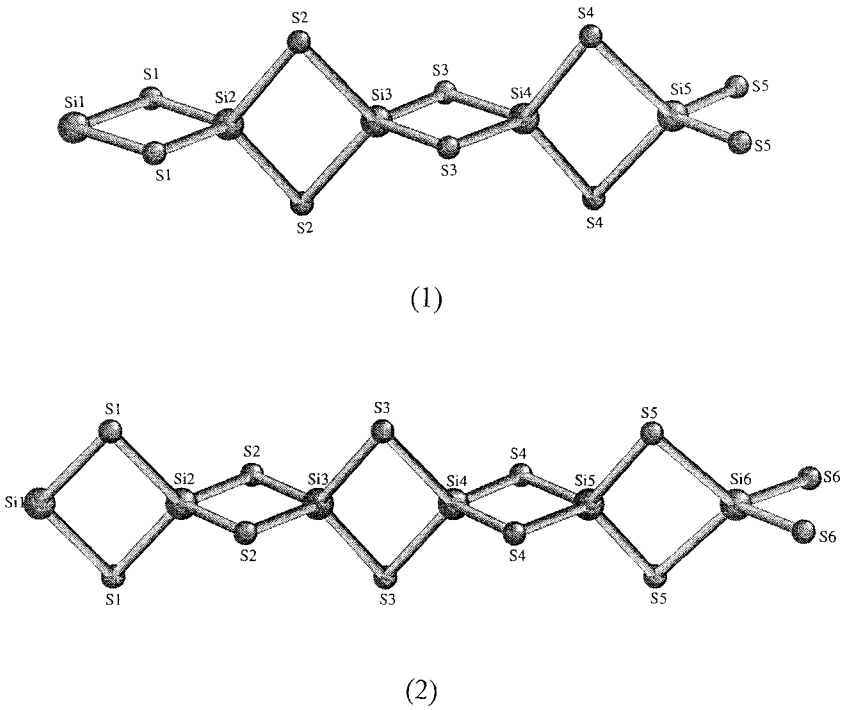

FIGURE 6. Geometrical structures of $(SiS_2)_5^-$, $(SiS_2)_6^-$ isomers.

with polarized and diffuse function 6-31+G* basis set. In general there are no severe discrepancies between the MP2 and B3LYP geometric parameters and the equilibrium geometry is close. Both MP2 and B3LYP include electron correction, but B3LYP is effective in larger cluster structure optimization, so we can conclude that the DFT approach is useful in establishing trends. In order to make a systemic study on the formation of $(SiS_2)_n^-$ (n = 1–6), our discussion is based on the result of DFT/B3LYP.

In Table III, we present the bond length, Mulliken charge on the equilibrium geometry of $(SiS_2)_n^-$ (n = 1–6) clusters. SiS_2^- as the core of $(SiS_2)_n^-$, there is a large negative charge on the S atoms, so when forming dimer, the reaction likely happen on the S atoms of SiS_2^- and the Si atom of SiS_2, for the net charge on the Si atom in SiS_2 is positive. The regularity of other oligomers formation is also like this. The conclusion can be inferred from the net charge of $(SiS_2)_2^-$, in all the oligomers, the net charge on terminal S atoms (denoted as $S_{(t)}$) is negative, and on terminal Si atom (denoted as $Si_{(t)}$) is positive. With the clusters chain growing, the bonds $Si_{(t)}$–S and $S_{(t)}$–Si change slightly, the bond length of $Si_{(t)}$–S is from 2.167 to 2.196 Å, and that of $S_{(t)}$–Si is from 2.075 to 2.064 Å. The bond length of Si–S in the cluster chain is almost similar, except the bond of the Si atom, which bind to $S_{(t)}$, and S atoms in chain (denoted as $S_{(b)}$); its bond length is from 2.230 to 2.251 Å. We conclude that decomposition reaction may happen in this position.

With the clusters chain growing, the net charge on terminal Si atom and terminal S atoms change slightly; on $Si_{(t)}$ it is from 0.25 to 0.35 (n = 3–6), and $S_{(t)}$ is from −0.30 to −0.26, and the charge on Si atom, which binds to $S_{(t)}$, is negative; we can conclude that the bond between terminal S atoms and Si atom is a stronger covalent bond, and the polarity is becoming weak with the clusters chain growing. The charge on the S atoms in the chain (denoted as $S_{(b)}$) is becoming smaller and smaller; on some S atoms it is less than ±0.01 [in $(SiS_2)_6^-$]. It is said that with the cluster growing, the polarity on the whole chain becomes great; the charge transfers to the terminal atoms.

In Table III, we present binding energies as well as average binding energies. The binding energy is defined as

$$E_b = E\left((SiS_2)_n^-\right) - nE(\mathrm{Si}) - 2nE(\mathrm{S}),$$

TABLE III

Symmetry, state, bond length, and Mulliken charge binding energy and average binding energy of $(SiS_2)_n^-$ (n = 1–6) optimized by B3LYP.

Clusters	Symmetry	State	Bond length (Å)	Mulliken charge	E_B (eV)	$\langle E_B \rangle$ (eV)
SiS_2^-	C_{2v}	$^2B_2$	Si–S 2.117	Si −0.0806 S −0.4597	10.3020	10.3020
$(SiS_2)_2^-$	C_{2v}	$^2B_1$	Si1–S1 2.167 Si2–S1 2.230 Si2–S2 2.075	Si1 −0.1670 Si2 −0.2228 S1 −0.1597 S2 −0.3124	21.9699	10.9850
$(SiS_2)_3^-$	C_{2v}	$^2B_2$	Si1–S1 2.179 Si2–S1 2.193 Si2–S2 2.115 Si3–S2 2.251 Si3–S3 2.068	Si1 0.2480 Si2 −0.3166 Si3 −0.1021 S1 −0.0931 S2 −0.0242 S3 −0.2973	33.3005	11.1002
$(SiS_2)_4^-$	C_{2v}	$^2A_2$	Si1–S1 2.186 Si2–S1 2.177 Si2–S2 2.129 Si3–S2 2.210 Si3–S3 2.112 Si4–S3 2.264 Si4–S4 2.076	Si1 0.3014 Si2 −0.4449 Si3 −0.0214 S4 −0.3151 S1 −0.0710 S2 −0.0334 S3 −0.0064 S4 −0.2160	44.2201	11.0550
$(SiS_2)_5^-$	C_{2v}	$^2B_2$	Si1–S1 2.193 Si2–S1 2.166 Si2–S2 2.138 Si3–S2 2.190 Si3–S3 2.126 Si4–S3 2.213 Si4–S4 2.109 Si5–S4 2.257 Si5–S5 2.065	Si1 0.3362 Si2 −0.3832 Si3 −0.1398 S4 0.0480 S5 −0.2607 S2 −0.0542 S2 −0.0387 S3 −0.0050 S4 −0.0173 S5 −0.2614	55.8010	11.1620
$(SiS_2)_6^-$	C_{2v}	$^2B_1$	Si1–S1 2.196 Si2–S1 2.160 Si2–S2 2.145 Si3–S2 2.179 Si3–S3 2.136 Si4–S3 2.193 Si4–S4 2.124 Si5–S4 2.215 Si5–S5 2.107 Si6–S5 2.258 Si6–S6 2.064	Si1 0.3509 Si2 −0.2980 Si3 −0.3004 Si4 −0.0900 Si5 −0.1393 Si6 −0.3006 S1 −0.0410 S2 0.0570 S3 0.0040 S4 −0.0058 S5 −0.0092 S6 −0.2557	66.9982	11.1664

where E is the total energy of the cluster or atom as indicated. The average binding energy is indicated as the binding energy of per unit in different cluster $(SiS_2)_n^-$.

The relative stability of these clusters can be better understood by calculating the energy gained by adding successive SiS_2 units to $(SiS_2)_n^-$ clusters. We define $\Delta E(n)$, the energy gain in adding a SiS_2

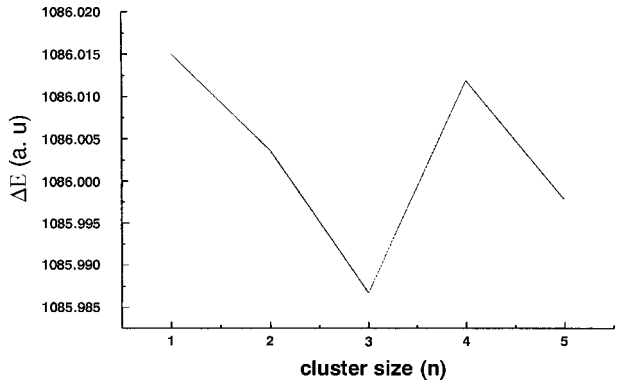

FIGURE 7. Plot of energy difference $\Delta E(n)$ as a function of cluster size n.

monomer to $(SiS_2)_n^-$ cluster, as

$$\Delta E(n) = -E(n+1) + E(n), \qquad n \geq 1.$$

In Figure 7 we plot $\Delta E(n)$ as a function of n. Note that the energy gain in adding SiS_2 to a $(SiS_2)_n^-$ cluster abruptly decrease from $n = 1$ to 3, and then vary nonmonotonically with clusters size, the energy is lower when $n = 3$ and 5, and higher at $n = 2$ and 4. It may indict that the stability regularity of the cluster has odd–even effect; the cluster that has odd units is more stable than even one.

The orbital energy of highest occupied molecular orbital (HOMO) and lowest unoccupied molecular orbital (LUMO), HOMO–LUMO gaps of $(SiS_2)_n^-$ are shown in Table IV. That the HOMO energy is rather low, and increases monotonically, it may indicate that the electron on the HOMO of SiS_2^- is more likely to lose. The HOMO–LUMO gaps in general decrease with the size of clusters increasing; this may indicate that the cluster $(SiS_2)_n^-$ has more activity in chemical reaction with the size increases.

In Table V, we present the vibrational frequencies of the most stable structure of $(SiS_2)_n^-$ clusters. From the analysis of the vibrational spectra of the clusters, the conclusion may be obtained that the most intense infrared vibrations are all a_1 symmetry, and the modes of the vibration are all Si atoms stretching vibrations along the molecular axis.

Conclusions

In summary, we have calculated the equilibrium geometry, energies, and electronic structure and vibrational spectra of $(SiS_2)_n^-$ ($n = 1$–6) clusters using the density function theory (DFT/B3LYP). We note that the most stable structures of $(SiS_2)_n^-$ have tetra-atomic ring chains of Si and S atoms bonded alternatively, and the rings are perpendicular to each other. It is predicted that the clusters growing trend of $(SiS_2)_n^-$ bases on the binding of Si and S atoms, with SiS_2^- as the core and SiS_2 as the unit. The bond of $Si–S_{(t)}$ in the clusters is strong covalent binding, and, with the cluster growing, the polarity on the whole chain become great and the charge transfers to the terminal atoms. We also predict the vibrational spectra of $(SiS_2)_n^-$ clusters, that the characteristic infrared absorb is Si atoms stretching vibration along the molecular chain, and the range is from 519 to 586 cm^{-1}.

ACKNOWLEDGMENTS

This work was financially supported by the National Natural Science Foundation of China. We thank Professor Zhang Hong Xing for his constructive suggestions.

TABLE IV
Molecular orbitals and orbital energies of the most stable isomer of $(SiS_2)_n^-$ ($n = 1$–6).

Cluster	Symmetry	State	Molecular orbital		Orbital energy		Energy gap
			HOMO	LUMO	HOMO	LUMO	
SiS_2^-	C_{2v}	$^2B_2$	a_1	b_2	−1.1143	−0.6539	0.4664
$(SiS_2)_2^-$	C_{2v}	$^2B_1$	a_2	b_1	−2.3804	−0.4348	1.9456
$(SiS_2)_3^-$	C_{2v}	$^2A_1$	a_2	b_2	−2.6969	−0.6150	2.0819
$(SiS_2)_4^-$	C_{2v}	$^2A_2$	b_1	b_1	−2.7121	−0.7159	1.9962
$(SiS_2)_5^-$	C_{2v}	$^2B_2$	a_2	b_1	−2.9409	−1.2517	1.6892
$(SiS_2)_6^-$	C_{2v}	$^2B_1$	a_2	b_1	−2.9910	−1.6106	1.3804

TABLE V

Normal-mode vibrational frequencies (cm^{-1}) of the most stable isomer of $(SiS_2)_n^-$ (n = 1–6) by B3LYP.[a]

Cluster	Symmetry	Vibrational frequencies			
SiS_2^-	C_{2v}	185/1.4(a_1)	418/14.1(b_2)	535/55.6(a_1)	
$(SiS_2)_2^-$	C_{2v}	75/0.0(b_1)	109/0.0(a_2)	138/3.1(a_1)	179/0.4(b_2)
		203/0.3(b_1)	252/6.4(a_1)	353/2.2(b_2)	379/21.4(a_1)
		491/107.7(a_1)	509/86.2(b_2)	520/1.3(b_1)	586/216.0(a_1)
$(SiS_2)_3^-$	C_{2v}	28/0.1(b_2)	66/0.2(b_1)	76/0.0(a_2)	116/0.0(a_2)
		121/3.4(a_1)	150/0.5(b_2)	165/1.4(b_1)	186/6.2(a_1)
		203/0.4(b_2)	215/0.0(b_1)	299/0.5(a_1)	361/15.2(b_1)
		362/50.5(a_1)	383/1.8(b_2)	406/37.9(a_1)	482/164.9(a_1)
		519/71.4(b_2)	530/0.4(b_2)	562/535.3(a_1)	588/78.1(b_1)
		600/4.4(a_1)			
$(SiS_2)_4^-$	C_{2v}	16/0.5(b_1)	23/0.3(b_2)	56/0.0 (a_2)	62/1.9(b_1)
		104/0.9(a_1)	105/0.0(a_2)	108/32.9(b_1)	128/0.0(a_2)
		134/1.1(b_2)	167/2.9(a_1)	178/3.7(b_1)	180/1.1(b_2)
		211/0.2(b_2)	212/2.6(b_1)	243/0.4(a_1)	322/12.3(a_1)
		256/11.8(b_2)	260/35.3(a_1)	388/5.5(b_2)	391/91.4(a_1)
		402/8.4(b_1)	414/36.5(a_1)	452/108.2(b_1)	476/248.7(a_1)
		519/484.2(a_1)	527/61.2(b_2)	562/376.3(a_1)	582.9/77.4(b_2)
		585.6/72.1(b_1)	599.3/0.9(a_1)		
$(SiS_2)_5^-$	C_{2v}	16/0.5(b_2)	17.5/0.6(b_1)	28/0.1 (b_2)	45/0.0(a_2)
		63/0.1(b_1)	83/0.0(a_2)	89/2.1(a_1)	108/0.0(a_2)
		113/0.0(a_2)	127/1.0(b_2)	130/0.1(b_1)	142/8.3(a_1)
		162/0.5(b_2)	172/1.9(b_1)	194/0.1(b_2)	199/0.1(a_1)
		202/0.1(b_1)	218/0.2(b_2)	222/0.3(b_1)	269/5.9(a_1)
		330/5.7(a_1)	356/14.2(b_1)	359/53.8(a_1)	389/6.8(b_2)
		390/45.8(a_1)	401/6.6(b_2)	405/110.0(a_1)	416/2.1(b_1)
		419/41.7(a_1)	471/278.4(a_1)	533/0.5(b_2)	534/59.5(b_2)
		537/1458.4(a_1)	577/0.9(a_1)	584/53.7(b_1)	588/66.2(b_2)
		593/84.7(b_1)	597/33.4(a_1)	608/0.1(a_1)	
$(SiS_2)_6^-$	C_{2v}	12/0.7(b_1)	13.5/0.7(b_2)	26/0.1 (b_1)	26/0.2(b_2)
		38/0.0(a_2)	62/0.1(b_1)	71/0.0(a_2)	77/1.8(a_1)
		96/0.0(a_2)	110/0.0(a_2)	113/0.0(a_2)	121/0.0(b_2)
		125/0.2(b_1)	130/8.1(a_1)	147/0.8(b_2)	157/1.7(b_1)
		174/0.7(a_1)	180/0.8(b_2)	186/0.3(b_1)	203/0.0(b_2)
		209/0.6(b_1)	220/0.1(b_2)	224/0.1(b_1)	233/4.0(a_1)
		290/0.5(a_1)	337/29.3(a_1)	354/14.2(b_2)	359.4/23.8(a_1)
		386/80.8(a_1)	388.8/9.4(b_2)	399/5.8(b_1)	401/59.5(a_1)
		412/111.6(a_1)	415/2.9(b_2)	422/44.4(a_1)	423/0.7(b_1)
		468/334.4(a_1)	528.6/2001.5(a_1)	534/2.9(b_1)	538/54.6(b_2)
		568/1.0(a_1)	584/32.7(b_1)	586/51.8(b_2)	589/100.1(b_1)
		589/48.8(a_1)	595/81.2(b_2)	602/1.0(a_1)	611/3.3(a_1)

[a] Frequency/IR intensity (symmetry), IR intensity in km/mol.

References

1. Raghavachari, K.; Rohlfing, C. M. J Chem Phys 1988, 89, 2219–2234.
2. Rohlfing, C. M.; Raghavachari, K. J Chem Phys 1992, 96, 2114–2117.
3. Kishi, R.; Iwata, S.; Nakajima, A.; Kaya, K. J Chem Phys 1997, 107, 3056–3070.
4. Kishi, R.; Kawamata, H.; Negishi, Y.; Iwata, S.; Nakajima, A.; Kaya, K. J Chem Phys 1997, 107, 10029–10043.
5. Kishi, R.; Negishi, Y.; Kawamata, H.; Iwata, S.; Nakajima, A.; Kaya, K. J Chem Phys 1998, 108, 8039–8058.

6. Harkless, J. A. W.; Stillinger, D. K.; Stillinger, F. H. J Phys Chem 1996, 100, 1098–1103.
7. Wang, L.-S.; Nicholas, J. B.; Dupuis, M.; Wu, H.-B.; Colson, S. D. Phys Rev Lett 1997, 78, 4450–4453.
8. Nayak, S. K.; Rao, B. K.; Khanna, S. N.; Jena, P. J Chem Phys 1998, 109, 1245–1250.
9. Hohl, D.; Jones, R. O.; Car, R.; Parrinello, M. J Chem Phys 1988, 89, 6823–6835.
10. Raghvachari, K.; Rohlfing, C. M.; Binkley, J. S. J Chem Phys 1990, 93, 5862–5874.
11. Sanov, A.; Lineberger, W. C.; Jordan, K. D. J Phys Chem 1998, 102, 2509–2511.
12. Meayama, T.; Oikawa, T.; Tohru, M. N. J Chem Phys 1998, 108, 1368–1376.
13. Bagatur'yants, A. A.; Safanov, A. A.; Stoll, H.; Werner, H.-J. J Chem Phys 1998, 109, 3096–3107.
14. Cui, M.; Feng, J.-K.; Ge, M.-F.; Wang, S.-F.; Sun, C.-C. Chem J Chinese Universities 1999, 20, 436–439.
15. Li, J.-Q.; Zhang, Y.-F.; Huang, Z.-X.; Wu, L. M.; Zhou, L.-X.; Lu, S.-F. Theochem 1998, 429, 237–246.
16. Hay, P. J.; Wadt, W. R. J Chem Phys 1985, 82, 270–283.
17. Wadt, W. R.; Hay, P. J. J Chem Phys 1985, 82, 284–298.
18. Hay, P. J.; Wadt, W. R. J Chem Phys 1985, 82, 299–310.
19. Ditchfield, R.; Hehre, W. J.; Pople, J. A. J Chem Phys 1971, 54, 724–728.
20. Hehre, W. J.; Ditchfield, R.; Pople, J. A. J Chem Phys 1972, 56, 2257–2261.
21. Hariharan, P. C.; Pople, J. A. Theo Chim Acta 1973, 28, 213–222.
22. Gordon, M. S. J Chem Phys 1980, 76, 163–172.
23. Hariharan, P. C.; Pople, J. A. Mol Phys 1974, 27, 209–215.
24. Frisch, M. J.; Trucks, G. W.; Schlegel, H. B.; Gill, P. M. W.; Johnson, B. G.; Robb, M. A.; Cheeseman, J. R.; Keith, T.; Petersson, G. A.; Montgomery, T. A.; Raghavachari, K.; Al-Laham, M. A.; Zakrzewski, V. G.; Ortiz, J. V.; Foresman, J. B.; Cioslowski, J.; Stefanov, B. B.; Nanayakkara, A.; Challacombe, M.; Peng, C. Y.; Ayala, P. Y.; Chen, W.; Wong, M. W.; Andres, J. L.; Replogle, E. S.; Gomperts, R.; Martin, R. L.; Fox, D. J.; Binkley, J. S.; Defrees, D. J.; Baker, J.; Stewart, J. P.; Head-Gordon, M.; Gonzalez, C.; Pople, J. A. Gaussian 94, Revision E.2; Gaussian: Pittsburgh, 1995.
25. King, R. A.; Galbraith, J. M.; Schaefer, H. F. J Phys Chem 1996, 100, 6061–6068.
26. Preilla-Márquez, J. D.; Rittby, C. M. L.; Graham, W. R. M. J Chem Phys 1997, 106, 8367–8373.
27. Redondo, P.; Sagüilo, A.; Largo, A. J Phys Chem 1998, 102, 3953–3958.
28. Bauschlicher, C. W.; Ricca, A. J Phys Chem 1998, 102, 4722–4727.